IRS-Aided Wideband Dual-Function Radar-Communications with Quantized Phase-Shifts

Tong Wei, Linlong Wu, Kumar Vijay Mishra, Bhavani Shankar M. R.
Interdisciplinary Centre for Security, Reliability and Trust (SnT), University of Luxembourg
email: {tong.wei@, linlong.wu@, kumar.mishra@ext., bhavani.shankar@}uni.lu

***Abstract*—Intelligent reflecting surface (IRS) are increasingly considered as an emerging technology to assist the wireless communications and target sensing. In this paper, we consider the quantized IRS-aided wideband dual-function radar-communications (DFRC) system with OFDM signaling. Specifically, the radar receive filter, frequency-dependent transmit beamforming and discrete phase-shifts are jointly designed to maximize the average signal-to-noise ratio (SINR) for radar while guaranteeing the communication SINR among all users. The resulting optimization problem, consisting of fractional quartic objective, difference of convex (DC) and discrete phase constraints, is highly nonconvex. Thus, we solve this problem via the alternating maximization (AM) framework, in which the alternating direction method of multipliers (ADMM) and Dinkelbach's algorithm are integrated to tackle the related subproblems. Numerical results demonstrate that the proposed method, even with the low-resolution IRS, achieves better sensing performance compared with no-IRS system.**

***Index Terms*—Alternating maximization, dual-function radar-communications, quantized-IRS, OFDM.**

I. Introduction

Several new technologies have been emerged in the next-generation wireless communication system, i.e., beyond 5G and 6G [1, 2]. For example, intelligent reflecting surface (IRS) which comprise many low-cost reconfigurable elements to control the phase of the impinging signal shows the superior ability to integrate into the different wireless applications and hence achieve the high date rate or the enhanced target localization [3–8]. Recently, dual-function radar-communications (DFRC) have been attracted a lot of research interest due to the special structure of the hardware resource and transmitted information sharing [9]. Combining the above features, IRS-assisted DFRC is developed to improve the communication quality and radar sensing, simultaneously [10, 11].

Notice that the initial investigations about IRS were proceeded in the wireless communications [12–16]. Generally, these works focus on deploying IRS to realize the passive beamforming in order to compensate the end-to-end path loss, i.e. transmitter-IRS and IRS-receiver channels. For example, in [15], IRS is utilized to estimate the position and orientation of user and then construct the channel state information (CSI) precisely. Further, under multi-IRS setting, the weighted sum-rate over all users is maximized while satisfying the constraint of total transmit power from the base-station [16]. Exploring the advantage of the intelligent spectrum control, some recent works utilize IRS to enhance the target localization and detection performance in multiple-input multiple-output (MIMO) radar system [5, 8, 17–19]. For example, in [17], the surface is closely deployed to the radar receive antennas in order to enhance the intensity of echo signals. Then, the passive beamforming can be well designed to maximize the receive signal-to-noise ratio (SNR). Similar as the non-line-of-sight (NLoS) communication, IRS can be also used to assist the NLoS radar detection and surveillance [19]. Based on above, we can conclude that IRS aims to provide the extra virtual line-of-sight (LoS) path between transmitter and receiver.

Compared with the coexistence schemes [20, 21], DFRC embeds the communication symbol into the transmitted signal and shares the same platform for both communication and sensing [22, 23]. Leveraging on the intelligent multi-beam control, IRS is also utilized in dual-function radar-communications (DFRC) to enhance the ability of sensing and/or communications [10, 11, 24, 25]. For example, in [24], the passive and active beamforming are jointly devised for the IRS-aided DFRC to enhance the radar detection performance while ensuring the single-user SNR. Further, in [11], the transmit waveform from dual-function base-station (DFBS) is designed to align the beam to the target directions. Then, the multi-user interference (MUI) is eliminated to guarantee the quality of service (QoS) with the assistance of IRS. Notice that the above mentioned works focus on the ideal IRS case in which the phase shifts of IRS are continuous. However, due to the hardware limitation, the practical phase takes the finite discrete value [26]. Different from the previous schemes [10, 11, 24], in this paper, we consider integrating IRS into wideband OFDM-DFRC system in which both the LoS and NLoS path are considered. Meanwhile, the quantized-IRS with discrete phase-shifts is considered to facilitate the implementation. By jointly designing the radar receive filter, transmit precoding matrix and discrete phase-shifts, the radar SINR are maximized while ensuring the communication SINR among single-antenna users. The resulting optimization problem is solved by the alternating maximization (AM) framework. Numerical results are provided to illustrate the effectiveness and superiority of the proposed design approach.

II. Signal Model

Let us consider an IRS-aided wideband OFDM-DFRC system consisting of a N_t-antenna dual-function transmitter, a N_r-antenna radar receiver and a single IRS comprising M reflecting elements, which aims to detect a target in presence of Q clutters while simultaneously serving U single-antenna

downlink (DL) users. We assume that the transmitter and receiver are composed of an uniform linear array (ULA) and closely deployed into the DFBS. Meanwhile, we consider both the direct (i.e., LoS) and indirect (i.e., NLoS) links for radar and communication systems. The transmit signal is composed of OFDM symbols, having the symbol duration $\triangle t$ and modulated to spread over K subcarriers. Denoting the normalized transmit data symbol at the k-th subcarrier as $\mathbf{s}_k = [s_{k,1}, \cdots, s_{k,U}]^T \in \mathbb{C}^{U\times 1}$, where $k = 1, \cdots, K$ and $\mathbb{E}\{\mathbf{s}_k\mathbf{s}_k^H\} = \mathbf{I}_U$. In this paper, we utilize the frequency-dependent digital beamforming $\mathbf{F}_k \in \mathbb{C}^{N_t\times U}$ to precode the data symbol in order to overcome beam-squint effect [27]. Utilizing the N_t K-point inverse fast Fourier transform (IFFT), the transmit baseband signal can be given by

$$\mathbf{x}(t) = \sum_{k=1}^{K} \mathbf{F}_k\mathbf{s}_k e^{j2\pi f_k t} \in \mathbb{C}^{N_t\times 1}, \tag{1}$$

where t denotes the time instant, $f_k = (k-1)\triangle f$ denotes the baseband frequency at the k-th subcarrier with $\triangle f$ being the frequency step of OFDM signaling. Meanwhile, the transmit power should satisfy

$$\|\mathbf{F}_k\|_F^2 \le \mathcal{P}_k, \tag{2}$$

where $\mathcal{P}_k$ denotes the maximum power assigned to the k-th subcarrier. Due to the hardware limitations, the phase-shifts of IRS should be discrete. Let B denotes the number of quantization bits of IRS and the discrete phase-shifts level

$$\mathcal{F} \triangleq \{\frac{2b\pi}{2^B} |\ b = 0, 1, \cdots, 2^B - 1\}. \tag{3}$$

A. Radar Model

Denote the frequency-dependent steering vectors of dual-function transmitter, radar receiver, and IRS, respectively, as

$$\begin{aligned}
\mathbf{a}_t(\theta, f_k) &= [1, e^{-jv(\theta,f_k)}, \cdots, e^{-j(N_t-1)v(\theta,f_k)}]^T,\\
\mathbf{a}_r(\theta, f_k) &= [1, e^{-jv(\theta,f_k)}, \cdots, e^{-j(N_r-1)v(\theta,f_k)}]^T,\\
\mathbf{b}(\theta, f_k) &= [1, e^{-jv(\theta,f_k)}, \cdots, e^{-j(M-1)v(\theta,f_k)}]^T,
\end{aligned}$$

where $v(\theta, f_k) = 2\pi(f_k + f_c)(\frac{d\sin(\theta)}{c})$. The target echo signal can be obtained from four different paths, i.e., Tx-target-Rx, Tx-IRS-target-Rx, Tx-target-IRS-Rx and Tx-IRS-target-IRS-Rx. After sampling the signal and applying K-point FFT, the radar received signal at the k-th subcarrier is given by

$$\mathbf{Y}(f_k) = \left(\mathbf{A}_k + \mathbf{P}_k(\mathbf{\Phi}) + \widetilde{\mathbf{A}}_k + \widetilde{\mathbf{P}}_k(\mathbf{\Phi})\right)\mathbf{F}_k\mathbf{s}_k + \mathbf{n}_r(f_k) \tag{4}$$

where $\mathbf{A}_k = \alpha_1\mathbf{a}_r(\theta, f_k)\mathbf{a}_t^T(\theta, f_k)$ denotes the target response matrix from Tx-target-Rx path, α_1 is the direct path gain, $\mathbf{P}_k(\mathbf{\Phi}) = \mathbf{E}_k\mathbf{\Phi}\mathbf{G}_k + \mathbf{D}_k\mathbf{\Phi}\mathbf{B}_k + \mathbf{D}_k\mathbf{\Phi}\mathbf{W}_k\mathbf{\Phi}\mathbf{G}_k$ denotes response matrix from the indirect paths, $\mathbf{G}_k$, $\mathbf{W}_k$, $\mathbf{D}_k$, $\mathbf{B}_k$ and $\mathbf{E}_k$ denote the channel matrix between Tx-IRS, IRS-IRS, IRS-Rx, Tx-target-IRS, IRS-target-Rx, respectively and $\mathbf{\Phi} = \mathrm{diag}(e^{j\phi_1}, \cdots, e^{j\phi_M}), \phi_m \in \mathcal{F}$ denotes the quantized phase-shifts matrix of IRS. Similarly, $\widetilde{\mathbf{A}}_k$ and $\widetilde{\mathbf{P}}_k$ denote the clutter response matrix for direct path and indirect path, respectively, wherein the steering vectors and angles are omitted due to the limited space. Based on (4), we can define the average SINR of radar over all subcarriers

$$\mathrm{SINR}_r = \frac{\sum_{k=1}^{K}|\mathbf{w}^H(\mathbf{A}_k + \mathbf{P}_k(\mathbf{\Phi}))\mathbf{F}_k\mathbf{s}_k|^2}{\sum_{k=1}^{K}|\mathbf{w}^H(\widetilde{\mathbf{A}}_k + \widetilde{\mathbf{P}}_k(\mathbf{\Phi}))\mathbf{F}_k\mathbf{s}_k|^2 + K\sigma_r^2\mathbf{w}^H\mathbf{w}}, \tag{5}$$

where $\mathbf{w}$ the receive filter bank and σ_r^2 denotes the noise power of radar at each subcarrier.

B. Communications Model

Denote the channel state information (CSI) matrices from transmitter and IRS to users on k-th subcarrier as $\mathbf{H}_k \in \mathbb{C}^{U\times N_t}$ and $\widetilde{\mathbf{H}}_k \in \mathbb{C}^{U\times M}$, respectively, in which the wideband channel model is adopted [28]. Meanwhile, we assume the CSI can be estimated in advance. Sampling the signal and applying K-point FFT, the receive signal of the u-th user at k-th subcarrier is given by

$$\begin{aligned}
\mathbf{Y}_u(f_k) &= \mathbf{h}_{u,k}^T\mathbf{f}_{k,u}s_{k,u} + \tilde{\mathbf{h}}_{u,k}^T\mathbf{\Phi}\mathbf{G}_k\mathbf{f}_{k,u}s_{k,u}\\
&+ \sum_{i\neq u}\mathbf{h}_{u,k}^T\mathbf{f}_{k,i}s_{k,i} + \sum_{i\neq u}\tilde{\mathbf{h}}_{u,k}^T\mathbf{\Phi}\mathbf{G}_k\mathbf{f}_{k,i}s_{k,i} + \mathbf{n}_u(f_k),
\end{aligned} \tag{6}$$

where $\mathbf{f}_{k,u}$ denotes the u-th column of $\mathbf{F}_k$, $\mathbf{n}_u(f_k)$ denotes the noise term for u-th user, $\mathbf{h}_{u,k}$ and $\tilde{\mathbf{h}}_{u,k}$ denote the transpose of u-th row of $\mathbf{H}_k$ and $\widetilde{\mathbf{H}}_k$, respectively. Based on (6), the average signal power of the u-th user over all K subcarriers can be expressed as

$$P_u = \sum_{k=1}^{K}\|\mathbf{z}_{u,k}(\mathbf{\Phi})\mathbf{F}_k\mathbf{\Lambda}_u\|_2^2, \tag{7}$$

where $\mathbf{z}_{u,k}(\mathbf{\Phi}) = \mathbf{h}_{u,k}^T + \tilde{\mathbf{h}}_{u,k}^T\mathbf{\Phi}\mathbf{G}_k$, $\mathbf{\Lambda}_u$ is the diagonal selection matrix with only the u-th element being one and the rest being zero. Meanwhile, the average power of multiuser interference (MUI) at the u-th user is

$$P_{MUI} = \sum_{k=1}^{K}\|\mathbf{z}_{u,k}(\mathbf{\Phi})\mathbf{F}_k\bar{\mathbf{\Lambda}}_u\|_2^2, \tag{8}$$

where $\bar{\mathbf{\Lambda}}_u$ is the diagonal matrix with only the u-th diagonal element being zero and the rest being one. Then, the SINR at the u-th users is directly given by

$$\mathrm{SINR}_u = \frac{\sum_{k=1}^{K}\|\mathbf{z}_{u,k}(\mathbf{\Phi})\mathbf{F}_k\mathbf{\Lambda}_u\|_2^2}{\sum_{k=1}^{K}\|\mathbf{z}_{u,k}(\mathbf{\Phi})\mathbf{F}_k\bar{\mathbf{\Lambda}}_u\|_2^2 + K\sigma_c^2}, \tag{9}$$

where σ_c^2 denotes the noise power of communications user which is constant over all subcarriers.

C. Problem Formulation

In order to improve both the sensing and communications performance, the radar SINR and the minimal communications SINR among all users should be maximized simultaneously. Mathematically, the optimization problem is formulated as

$$\begin{aligned}
\underset{\mathbf{w},\mathbf{\Phi},\mathbf{F}_k}{\text{maximize}} \quad & \mathrm{SINR}_r\\
\text{subject to} \quad & \mathrm{SINR}_u \ge t, \forall u,\\
& \|\mathbf{F}_k\|_F^2 \le \mathcal{P}_k, \forall k,\\
& |\mathbf{\Phi}(i,i)| = 1, \arg\{\mathbf{\Phi}(i,i)\} \in \mathcal{F}, \forall i,
\end{aligned} \tag{10}$$

where $\mathcal{P}_k$ denotes the maximal transmit power at k-th subcarrier and t denotes the SINR threshold for communication users. Problem (10) which consists of fractional quartic objective function, constant modulus and difference of convex (DC) constraints, is highly nonconvex. To tackle problem (10), an alternating maximization (AM) based approach will is devised in the sequel.

III. Optimization method

In this section, we utilize the AM framework to decouple and simplify the transmit beamforming, receive filter and phase-shifts matrix design.

A. Update of receive filter $\mathbf{w}$

For the given transmit beamforming $\mathbf{F}_k$ and phase-shifts $\mathbf{\Phi}$, the subproblem w.r.t receive filter bank $\mathbf{w}$ can be expressed as

$$\underset{\mathbf{w}}{\text{maximize}} \ \frac{\mathbf{w}^H \mathbf{\Upsilon}_t \mathbf{w}}{\mathbf{w}^H \mathbf{\Upsilon}_c \mathbf{w} + K\sigma_r^2 \mathbf{w}^H \mathbf{w}}, \tag{11}$$

where

$$\begin{aligned} \mathbf{\Upsilon}_t &= \sum_{k=1}^{K} (\mathbf{A}_k + \mathbf{P}_k(\mathbf{\Phi}))\mathbf{F}_k \mathbf{F}_k^H (\mathbf{A}_k + \mathbf{P}_k(\mathbf{\Phi}))^H, \\ \mathbf{\Upsilon}_c &= \sum_{k=1}^{K} (\widetilde{\mathbf{A}}_k + \widetilde{\mathbf{P}}_k(\mathbf{\Phi}))\mathbf{F}_k \mathbf{F}_k^H (\widetilde{\mathbf{A}}_k + \widetilde{\mathbf{P}}_k(\mathbf{\Phi}))^H. \end{aligned} \tag{12}$$

Notice that problem (11) consists of fractional quadratic programming which is different from the conventional the minimum variance distortionless response (MVDR). Hence, the Charnes-Cooper transformation can be used to reformulate problem (12) as

$$\begin{aligned} \underset{\mathbf{w}}{\text{minimize}} \quad & \mathbf{w}^H \widetilde{\mathbf{\Upsilon}}_c \mathbf{w} \\ \text{subject to} \quad & \mathbf{w}^H \mathbf{\Upsilon}_t \mathbf{w} = 1 \end{aligned} \tag{13}$$

where $\widetilde{\mathbf{\Upsilon}}_c = \mathbf{\Upsilon}_c + K\sigma_r^2 \mathbf{I}$. It is seen that problem (13) consists of the complex-valued homogeneous QCQP which is nonconvex due to the quadratic equality constraint.

Lemma 1: For the function $f(\mathbf{x}) = \mathbf{x}^H \mathbf{H} \mathbf{x}$, the following inequalities are satisfied

$$f(\mathbf{x}) \geq 2\Re(\mathbf{x}_n^H \mathbf{H} \mathbf{x}) - f(\mathbf{x}_n), \tag{14a}$$

$$f(\mathbf{x}) \leq 2\Re(\mathbf{x}_n^H (\mathbf{H} - \xi \mathbf{I})\mathbf{x}) + 2\xi N - f(\mathbf{x}_n), \tag{14b}$$

where $\mathbf{H}$ is a semidefinite Hermitian matrix, N is the length of $\mathbf{x}$, $\xi \geq \lambda_{\max}(\mathbf{H})$, $\mathbf{x}_n$ denotes the current point and the second inequality (14b) holds only if $\mathbf{x}^H \mathbf{x} = N$.

Based on (14a), problem (13) can be reformulated

$$\begin{aligned} \underset{\mathbf{w}}{\text{minimize}} \quad & \mathbf{w}^H \widetilde{\mathbf{\Upsilon}}_c \mathbf{w} \\ \text{subject to} \quad & 2\Re(\mathbf{w}_n^H \mathbf{\Upsilon}_t \mathbf{w}) = 1 + \mathbf{w}_n^H \mathbf{\Upsilon}_t \mathbf{w}_n, \end{aligned} \tag{15}$$

where $\mathbf{w}_n$ denotes the value in previous iteration. Noted that problem (15) can be solved via CVX.

B. Update of precoding matrices $\mathbf{F}_k$

With the fixed $\mathbf{w}$ and $\mathbf{\Phi}$, the corresponding optimization problem can be written as

$$\begin{aligned} \underset{\boldsymbol{f} \in \mathbb{C}^{KN_tU \times 1}}{\text{maximize}} \quad & \frac{\boldsymbol{f}^H \mathbf{\Xi}_t \boldsymbol{f}}{\boldsymbol{f}^H \mathbf{\Xi}_c \boldsymbol{f} + K\sigma_r^2 \mathbf{w}_p^H \mathbf{w}_p} \\ \text{subject to} \quad & \|\mathbf{V}_k \boldsymbol{f}\|_2^2 \leq P_k, \forall k, \\ & \frac{\boldsymbol{f}^H \mathbf{R}_u \boldsymbol{f}}{\boldsymbol{f}^H \bar{\mathbf{R}}_u \boldsymbol{f} + K\sigma_c^2} \geq t, \forall u, \end{aligned} \tag{16}$$

where $\boldsymbol{f} = [\mathrm{vec}(\mathbf{F}_1)^T, \cdots, \mathrm{vec}(\mathbf{F}_K)^T]^T$, $\mathbf{V}_k$ denotes the selection matrix to extract k-th interval of $\boldsymbol{f}$. Due to space limitation, we omit the the detailed expression of semidefinite matrices $\mathbf{\Xi}_t$, $\mathbf{\Xi}_c$, $\mathbf{R}_u$ and $\bar{\mathbf{R}}_u$ which can be directly derived from (4) and (9). According to the inequality (14a), we can linearize and reformulate the objective function and constraint of problem (16) as

$$\begin{aligned} \underset{\boldsymbol{f}}{\text{maximize}} \quad & \frac{2\Re(\boldsymbol{f}_n^H \mathbf{\Xi}_t \boldsymbol{f}) - \boldsymbol{f}_n^H \mathbf{\Xi}_t \boldsymbol{f}_n}{\boldsymbol{f}^H \mathbf{\Xi}_c \boldsymbol{f} + K\sigma_r^2 \mathbf{w}^H \mathbf{w}} \\ \text{subject to} \quad & \|\mathbf{V}_k \boldsymbol{f}\|_2^2 \leq \mathcal{P}_k, \forall k, \\ & \xi \boldsymbol{f}^H \bar{\mathbf{R}}_u \boldsymbol{f} - 2\Re(\boldsymbol{f}_n^H \mathbf{R}_u \boldsymbol{f}) \leq const., \forall u \end{aligned} \tag{17}$$

where $const. = -\xi K\sigma_c^2 - \boldsymbol{f}_n^H \mathbf{R}_u \boldsymbol{f}_n$ and $\boldsymbol{f}_n$ denotes the value in last iteration. Noticed that problem (17) can be solved by Dinkelbach's algorithm [29].

C. Update of phase shift matrix $\mathbf{\Phi}$

With the fixed $\mathbf{w}$ and $\mathbf{F}_k$, the corresponding optimization problem can be written as

$$\begin{aligned} \underset{\boldsymbol{\phi}}{\text{maximize}} \quad & \frac{\bar{f}(\boldsymbol{\phi})}{\bar{g}(\boldsymbol{\phi})} \\ \text{subject to} \quad & |\boldsymbol{\phi}_i| = 1, \arg(\boldsymbol{\phi}_i) \in \mathcal{F}, \forall i \\ & \frac{q_u + 2\Re\{\boldsymbol{\phi}^H \mathbf{q}_u\} + \boldsymbol{\phi}^H \mathbf{Q}_u \boldsymbol{\phi}}{\bar{q}_u + 2\Re\{\boldsymbol{\phi}^H \bar{\mathbf{q}}_u\} + \boldsymbol{\phi}^H \bar{\mathbf{Q}}_u \boldsymbol{\phi} + K\sigma_c^2} \geq t, \forall u, \end{aligned} \tag{18}$$

where $\boldsymbol{\phi} = \mathrm{diag}(\mathbf{\Phi})$, $\bar{f}(\boldsymbol{\phi})$ and $\bar{g}(\boldsymbol{\phi})$ are quartic over the variable $\boldsymbol{\phi}$. Hence, the auxiliary variable $\boldsymbol{\psi}$ is introduced to reformulate problem (18) as

$$\begin{aligned} \underset{\boldsymbol{\phi}, \boldsymbol{\psi}}{\text{maximize}} \quad & \bar{f}(\boldsymbol{\phi}, \boldsymbol{\psi}) - \bar{\lambda} \bar{g}(\boldsymbol{\phi}, \boldsymbol{\psi}) \\ \text{subject to} \quad & \boldsymbol{\phi} = \boldsymbol{\psi} \\ & |\boldsymbol{\phi}(i)| = 1, |\boldsymbol{\psi}(i)| = 1, \forall i \\ & 2\Re(\mathbf{r}_u^H \boldsymbol{\phi}) \leq d_u, \forall u, \end{aligned} \tag{19}$$

where $\mathbf{r}_u = (\xi \boldsymbol{\phi}_n^H (\bar{\mathbf{Q}}_u - \eta_u \mathbf{I}) + \xi \bar{\mathbf{q}}_u^H - \mathbf{q}_u^H - \boldsymbol{\phi}_n^H \mathbf{Q}_u)^H$, η_u is the largest eigenvalue of $\bar{\mathbf{Q}}_u$, $d_u = \xi(\bar{q}_u + K\sigma_c^2 - 2\eta MN_m + \boldsymbol{\phi}_n^H \bar{\mathbf{Q}}_u \boldsymbol{\phi}_n) + \boldsymbol{\phi}_n^H \mathbf{Q}_u \boldsymbol{\phi}_n - q_u$, $\boldsymbol{\phi}_n$ denotes the current point of $\boldsymbol{\phi}$, $\bar{f}(\boldsymbol{\phi}, \boldsymbol{\psi})$ and $\bar{g}(\boldsymbol{\phi}, \boldsymbol{\psi})$ are given by

$$\bar{f}(\boldsymbol{\phi}, \boldsymbol{\psi}) = \boldsymbol{\phi}^H \mathbf{E} \boldsymbol{\phi} + 2\Re(\boldsymbol{\phi}^H \mathbf{e}) + e = \boldsymbol{\psi}^H \hat{\mathbf{E}} \boldsymbol{\psi} + 2\Re(\boldsymbol{\psi}^H \hat{\mathbf{e}}) + \hat{e},$$

$$\bar{g}(\boldsymbol{\phi}, \boldsymbol{\psi}) = \boldsymbol{\phi}^H \mathbf{Z} \boldsymbol{\phi} + 2\Re(\boldsymbol{\phi}^H \mathbf{z}) + z = \boldsymbol{\psi}^H \hat{\mathbf{Z}} \boldsymbol{\psi} + 2\Re(\boldsymbol{\psi}^H \hat{\mathbf{z}}) + \hat{z}.$$

Then, the augmented Lagrangian function of (19) is given by

$$\mathcal{L}(\boldsymbol{\phi},\boldsymbol{\psi},\mathbf{u},\mathbf{w},\rho) = f(\boldsymbol{\phi},\boldsymbol{\psi},\bar{\lambda}) - \Re(\mathbf{u}^H(\boldsymbol{\phi}-\boldsymbol{\psi})) - \frac{\rho}{2}\|\boldsymbol{\phi}-\boldsymbol{\psi}\|_2^2 - \sum_{u=1}^{U} w_u(2\Re(\mathbf{r}_u^H\boldsymbol{\phi}) - d_u), \tag{20}$$

where $f(\boldsymbol{\phi},\boldsymbol{\psi},\bar{\lambda}) = \bar{f}(\boldsymbol{\phi},\boldsymbol{\psi}) - \bar{\lambda}\bar{g}(\boldsymbol{\phi},\boldsymbol{\psi})$, ρ is the penalty parameter, $\mathbf{u}$ and $\mathbf{w} \succeq \mathbf{0}$ denote the auxiliary variables. According to (14a) and (14b), we can linearize $f(\boldsymbol{\phi},\boldsymbol{\psi},\bar{\lambda})$ and then rewrite (20) as $\bar{\mathcal{L}}(\boldsymbol{\phi},\boldsymbol{\psi},\mathbf{u},\mathbf{w},\rho)$. Based on above, the consensus-ADMM update formulas are given by

$$\bar{\lambda}^{(t+1)} = \frac{\bar{f}(\boldsymbol{\phi})}{\bar{g}(\boldsymbol{\phi})}, \tag{21a}$$

$$\boldsymbol{\phi}^{(t+1)} = \arg\max_{\boldsymbol{\phi}\in\mathcal{F}} \mathcal{L}(\bar{\lambda}^{(t+1)},\boldsymbol{\phi},\boldsymbol{\psi}^{(t)},\mathbf{u}^{(t)},\mathbf{v}^{(t)}), \tag{21b}$$

$$\boldsymbol{\psi}^{(t+1)} = \arg\max_{\boldsymbol{\psi}\in\mathcal{F}} \mathcal{L}(\bar{\lambda}^{(t+1)},\boldsymbol{\phi}^{(t+1)},\boldsymbol{\psi},\mathbf{u}^{(t)},\mathbf{v}^{(t)}), \tag{21c}$$

$$\mathbf{u}^{(t+1)} = \mathbf{u}^{(t)} + \rho_1(\boldsymbol{\phi}^{(t+1)} - \boldsymbol{\psi}^{(t+1)}), \tag{21d}$$

$$w_u^{(t+1)} = \mathrm{Proj}_+(w_u^{(t)} - (2\Re(\mathbf{r}_u^H\boldsymbol{\phi}) - d_u)), \forall u. \tag{21e}$$

Notice that the discrete-phase linear programming (LP) sub-problem (21b) and (21c) can be simplified and divided as

$$\begin{aligned} \underset{x_i}{\text{maximize}} \quad & \cos(x_i - \arg\{y_i\}) \\ \text{subject to} \quad & x_i \in \mathcal{F}. \end{aligned} \tag{22}$$

Then, problem (22) can be solved via the method [30].

IV. Numerical Experiments

Throughout the simulations, we assume both the dual-function transmitter and radar receiver are equipped with the ULA with $N_t = 6$ and $N_r = 4$ elements, respectively, and located at $[0, 0]$ in 2-D Cartesian plane. A single target is located at 0°. Two clutters is from 15° and -25°. We assume that IRS consists of $M = 30$ reflecting elements is deployed at $[2500, 2500]$ to assist the DFRC system, i.e., 45°. The central frequency of the wideband DFRC is 10 GHz and the subcarrier step-size is set as 200 MHz. Meanwhile, we set $K = 32$ and $U = 2$, respectively. The related element spacing for the transmitter, radar receiver and IRS are set according to the highest frequency, i.e., $d = c/2f_{max}$. The transmit power constraints at all subcarriers are set as identical, i.e., $P_1 = \cdots, = P_K = 1$. The beamforming matrices $\mathbf{F}_k$ and phase-shifts matrices $\boldsymbol{\Phi}$ are initialized with the diagonal entries generated from a zero-mean Gaussian distribution. We set the minimum value for communication SINR as $t = 8$. The maximum iteration for both inner-loop and out-loop are set as 30 times.

Fig.1 shows the achievable radar SINR versus the number of iterations. It is seen that the proposed algorithm converges within around 12 iterations. Obviously, IRS-aided DFRC can obtain the higher radar SINR. Meanwhile, as the increasing of bit number of IRS, the better radar performance is achieved which caused by the larger feasible set. However, the hardware complexity of IRS will also increased. Thus, the radar system performance and design complexity should be well balanced in real application.

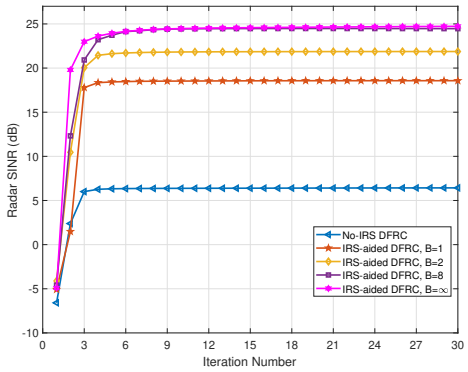

Figure 1. Radar SINR versus number of iterations.

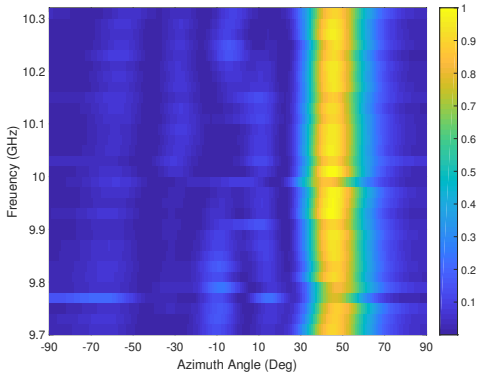

Figure 2. Illustration of wideband transmit beampattern.

Fig.2 shows the wideband transmit beampattern of the dual-function transmitter. It is seen that the transmit energy is almost totally focused on the direction of IRS. This is because that three indirect links (i.e., IRS-aided channels) can achieve higher channel gain compared with direct link. Based on above, we conclude that the proposed method can automatically align the transmit beam to the direction target or IRS, depended on which channel gain higher.

V. Summary

In this paper, we consider the quantized-IRS-aided wideband OFDM-DFRC system in which both the LoS and NLoS paths are existed. The frequency-dependent transmit beamforming is utilized to against the beam-squint effect. By properly designing, the radar receive filter, transmit beamforming and discrete phase-shifts matrix, the average radar SINR is maximized while ensuring the communication SINR among users. The resulting optimization consisting of fractional quartic objective function and discrete pahse constraints is highly nonconvex. Hence, an alternating maximization (AM) based algorithm is developed to tackle it. Simulation results shows that the proposed method can achieve satisfactory performance compared with no-IRS case.

REFERENCES

[1] E. Basar, "Reconfigurable intelligent surface-based index modulation: A new beyond MIMO paradigm for 6g," *IEEE Transactions on Communications*, vol. 68, no. 5, pp. 3187–3196, 2020.

[2] J. A. Hodge, K. V. Mishra, and A. I. Zaghloul, "Intelligent time-varying metasurface transceiver for index modulation in 6G wireless networks," *IEEE Antennas and Wireless Propagation Letters*, vol. 19, no. 11, pp. 1891–1895, 2020.

[3] M. Di Renzo, A. Zappone, M. Debbah, M.-S. Alouini, C. Yuen, J. de Rosny, and S. Tretyakov, "Smart radio environments empowered by reconfigurable intelligent surfaces: How it works, state of research, and the road ahead," *IEEE Journal on Selected Areas in Communications*, vol. 38, no. 11, pp. 2450–2525, 2020.

[4] Q. Wu and R. Zhang, "Towards smart and reconfigurable environment: Intelligent reflecting surface aided wireless network," *IEEE Communications Magazine*, vol. 58, no. 1, pp. 106–112, 2020.

[5] S. Buzzi, E. Grossi, M. Lops, and L. Venturino, "Radar target detection aided by reconfigurable intelligent surfaces," *IEEE Signal Processing Letters*, vol. 28, pp. 1315–1319, 2021.

[6] C. Huang, A. Zappone, G. C. Alexandropoulos, M. Debbah, and C. Yuen, "Reconfigurable intelligent surfaces for energy efficiency in wireless communication," *IEEE Transactions on Wireless Communications*, vol. 18, no. 8, pp. 4157–4170, 2019.

[7] M. F. Ahmed, K. P. Rajput, N. Venkategowda, K. V. Mishra, and A. K. Jagannatham, "Joint transmit and reflective beamformer design for secure estimation in IRS-aided WSNs," *IEEE Signal Processing Letters*, vol. 29, pp. 692–696, 2022.

[8] Z. Esmaeilbeig, K. V. Mishra, and M. Soltanalian, "IRS-aided radar: Enhanced target parameter estimation via intelligent reflecting surfaces," 2021.

[9] Z. Cheng, Z. He, and B. Liao, "Hybrid beamforming design for OFDM dual-function radar-communication system," *IEEE Journal of Selected Topics in Signal Processing*, vol. 15, no. 6, pp. 1455–1467, 2021.

[10] K. V. Mishra, A. Chattopadhyay, S. S. Acharjee, and A. P. Petropulu, "OptM3Sec: Optimizing multicast IRS-aided multiantenna DFRC secrecy channel with multiple eavesdroppers," in *IEEE International Conference on Acoustics, Speech and Signal Processing*, 2022, in press.

[11] X. Wang, Z. Fei, Z. Zheng, and J. Guo, "Joint waveform design and passive beamforming for RIS-assisted dual-functional radar-communication system," *IEEE Transactions on Vehicular Technology*, vol. 70, no. 5, pp. 5131–5136, 2021.

[12] J. Liu, X. Qian, and M. Di Renzo, "Interference analysis in reconfigurable intelligent surface-assisted multiple-input multiple-output systems," in *IEEE International Conference on Acoustics, Speech and Signal Processing*, 2021, pp. 8067–8071.

[13] M. Najafi, V. Jamali, R. Schober, and H. V. Poor, "Physics-based modeling and scalable optimization of large intelligent reflecting surfaces," *IEEE Transactions on Communications*, vol. 69, no. 4, pp. 2673–2691, 2021.

[14] Z. Zhou, N. Ge, Z. Wang, and L. Hanzo, "Joint transmit precoding and reconfigurable intelligent surface phase adjustment: A decomposition-aided channel estimation approach," *IEEE Transactions on Communications*, vol. 69, no. 2, pp. 1228–1243, 2021.

[15] A. Elzanaty, A. Guerra, F. Guidi, and M.-S. Alouini, "Reconfigurable intelligent surfaces for localization: Position and orientation error bounds," *IEEE Transactions on Signal Processing*, vol. 69, pp. 5386–5402, 2021.

[16] Z. Li, M. Hua, Q. Wang, and Q. Song, "Weighted sum-rate maximization for multi-IRS aided cooperative transmission," *IEEE Wireless Communications Letters*, vol. 9, no. 10, pp. 1620–1624, 2020.

[17] W. Lu, B. Deng, Q. Fang, X. Wen, and S. Peng, "Intelligent reflecting surface-enhanced target detection in MIMO radar," *IEEE Sensors Letters*, vol. 5, no. 2, pp. 1–4, 2021.

[18] W. Lu, Q. Lin, N. Song, Q. Fang, X. Hua, and B. Deng, "Target detection in intelligent reflecting surface aided distributed MIMO radar systems," *IEEE Sensors Letters*, vol. 5, no. 3, pp. 1–4, 2021.

[19] A. Aubry, A. De Maio, and M. Rosamilia, "Reconfigurable intelligent surfaces for N-LOS radar surveillance," *IEEE Transactions on Vehicular Technology*, vol. 70, no. 10, pp. 10 735–10 749, 2021.

[20] J. Qian, M. Lops, L. Zheng, X. Wang, and Z. He, "Joint system design for coexistence of MIMO radar and MIMO communication," *IEEE Transactions on Signal Processing*, vol. 66, no. 13, pp. 3504–3519, 2018.

[21] T. Wei, L. Wu, and B. Shankar M. R., "Joint waveform and precoding design for coexistence of MIMO radar and MU-MISO communication," *IET Signal Processing*, 2022, in press.

[22] K. V. Mishra, B. Shankar M. R., V. Koivunen, B. Ottersten, and S. A. Vorobyov, "Toward millimeter-wave joint radar communications: A signal processing perspective," *IEEE Signal Processing Magazine*, vol. 36, no. 5, pp. 100–114, 2019.

[23] T. Tian, T. Zhang, L. Kong, and Y. Deng, "Transmit/receive beamforming for MIMO-OFDM based dual-function radar and communication," *IEEE Transactions on Vehicular Technology*, vol. 70, no. 5, pp. 4693–4708, 2021.

[24] Z.-M. Jiang, M. Rihan, P. Zhang, L. Huang, Q. Deng, J. Zhang, and E. M. Mohamed, "Intelligent reflecting surface aided dual-function radar and communication system," *IEEE Systems Journal*, pp. 1–12, 2021.

[25] R. S. P. Sankar, B. Deepak, and S. P. Chepuri, "Joint communication and radar sensing with reconfigurable intelligent surfaces," *arXiv*, 2021.

[26] Z. Sun and Y. Jing, "On the performance of multi-antenna irs-assisted noma networks with continuous and discrete irs phase shifting," *IEEE Transactions on Wireless Communications*, pp. 1–1, 2021.

[27] M. Wang, F. Gao, S. Jin, and H. Lin, "An overview of enhanced massive MIMO with array signal processing techniques," *IEEE Journal of Selected Topics in Signal Processing*, vol. 13, no. 5, pp. 886–901, 2019.

[28] H. Li, M. Li, Q. Liu, and A. L. Swindlehurst, "Dynamic hybrid beamforming with low-resolution pss for wideband mmwave mimo-ofdm systems," *IEEE Journal on Selected Areas in Communications*, vol. 38, no. 9, pp. 2168–2181, 2020.

[29] A. Aubry, A. De Maio, and M. M. Naghsh, "Optimizing radar waveform and doppler filter bank via generalized fractional programming," *IEEE Journal of Selected Topics in Signal Processing*, vol. 9, no. 8, pp. 1387–1399, 2015.

[30] X. Yu, G. Cui, J. Yang, J. Li, and L. Kong, "Quadratic optimization for unimodular sequence design via an ADPM framework," *IEEE Transactions on Signal Processing*, vol. 68, pp. 3619–3634, 2020.